On the applicability of the single parabolic band model to advanced thermoelectric materials with complex band structures

Johannes de Boor[*]

Institute of Materials Research, German Aerospace Center (DLR), 51147 Koeln, Germany
E-mail: Johannes.deboor@dlr.de

Abstract

Due to the complex interplay between composition, synthesis parameters and the performance of thermoelectric materials, the optimization of thermoelectric materials needs to be complemented by modelling. A relatively simple and thus popular approach is the so called single parabolic band model, which allows for an efficient optimization of the material properties and a benchmarking of different materials based on relatively few, well available experimental results. As complex band structures are common for high performance materials, single parabolic band modelling is also employed with apparent success for material systems the underlying assumptions are not well fulfilled. In order to assess the validity of a single parabolic band analysis for such systems, the thermoelectric properties for two model systems are calculated: one with a single band that is twofold degenerate and one with a light and a heavy band. Even if the density of states masses and are kept identical, the transport properties and in particular the Hall coefficients differ significantly, which leads to an incorrectly determined carrier concentration. As the carrier concentration is the base for the single parabolic band analysis, all the quantities obtained from it (optimum carrier concentration, effective mass, deformation potential) are determined incorrectly as well.

1. Introduction

Thermoelectric materials are very attractive as they can directly convert waste heat into electricity. Thermoelectric systems have advantages such as small system size, no moving parts, heating and cooling options employed in a single system, environmental compatibility and high reliability. The development of thermoelectric generators (TEG) is promising for a range of diverse applications, ranging from self-powering sensors to waste heat recovery in the automotive sector and the steel industry. Further applications include the powering of space probes or extraterrestrial vehicles [1-3]. The efficiency of thermoelectric generators depends on the figure of merit zT of the employed materials, which is defined by $zT = \frac{S^2\sigma}{\kappa} T$, where S is the Seebeck coefficient, σ the electrical conductivity, κ the thermal conductivity, and T the temperature. All thermoelectric transport properties depend on the carrier concentration n of the material [2]. As materials with good thermoelectric properties can be obtained from a large number of elements, the compositional parameter space is basically unlimited. This means that efficient material optimization cannot be done experimentally only, but needs to be complemented by modelling efforts; be it to optimize a given material with respect to carrier concentration or to compare different material systems. *Ab initio* calculations are becoming ever more powerful in predicting thermoelectric performance, e.g. by employing DFT to calculate electronic band structures and using the Boltzmann Transport Equation (BTE) to calculate electronic and phononic transport [4-7]. Recently, machine learning and

high-throughput approaches are also used to identify promising TE materials [8-10]. However, these and similar approaches first still require experimental verification and secondly, are not always best for understanding the rationale behind the calculated properties. For experimental material developers on the other hand, simplified models based on the BTE are very popular[11-15]. Probably the simplest approach is the so-called single parabolic band (SPB) model which describes the electronic transport properties based on a single parabolic band with a single effective mass [16-21]. The power and the beauty of this model lies in the fact that a complete description of the model system can be obtained from relatively few and accessible experimental quantities: σ, S, κ and the Hall carrier concentration n_H. As the SPB naturally disregards the influence of minority carriers it is well known to have significant shortcomings, especially at higher temperatures [22-24]. Also, if the contribution of several bands varies with temperature due to a temperature dependent band structure, the necessity to use more than one band for a description of the material has been recognized [23, 25]. Still, within the SPB model a straightforward prediction of the optimum carrier concentration can be obtained relatively easily which shows decent agreement with experimental data, see e.g. [26, 27]. Furthermore, more fundamental material parameters can be derived from the SPB modelling allowing for a systematic comparison of different material classes and hence a rational selection of the better material or identification of the best composition in a range of solid solutions [28, 29]. As the use and the evaluation of the SPB model is so simple it has also been applied with apparent success to material systems where the fundamental assumption of one dominant parabolic band is not well fulfilled. A noteworthy example is n-$Mg_2Si_{1-x}Sn_x$ with $x \approx 0.65$ where the two lowest lying conduction bands with different curvatures have the same energetic minimum, see [30-33]. Liu et al. with their work, "Advanced thermoelectrics governed by a single parabolic band: $Mg_2Si_{0.3}Sn_{0.7}$, a canonical example", in particular, emphasize that the transport of that material can be described very well using a SPB model [34]. Other material systems are p-Mg_2X [26, 35, 36], where, in fact, 2 or three valence bands are relevant [37], PbTe [38-40] Si [41-43], Mg_3Sb_2 based compounds [44, 45], and half-Heuslers [46].

In reality, energetically degenerate bands as well as bands with dissimilar masses are features that favor good thermoelectric properties [39, 47, 48]. Therefore band structures more complex than a single parabolic band are rather the norm than the exception in good thermoelectric materials. While the SPB model is often applied for these material systems, the inaccuracies that arise due to not having a single parabolic band in practice are unknown and often usually neglected. In this work we will compare the transport properties of a model system that strictly follows the SPB model with one that has two bands with distinct properties and discuss the arising differences. We will also analyze the errors that arise if the two band system is treated in a SPB approach. Depending on the difference in band mass between the two bands the errors can be significant and can lead to largely incorrectly estimated material properties.

2. Calculation

Let us first consider the basic equations for a single parabolic band system[16, 49]. We'll assume that scattering of acoustic phonons is the dominant scattering mechanism (scattering parameter $\lambda = 0$) as this is typically observed for thermoelectric materials at room temperature or above.

The carrier concentration n is related to the density of states effective mass m_D^* and the reduced chemical potential $\eta = \frac{E_\mathrm{F}}{k_B T}$, ($E_\mathrm{F}$ is the Fermi energy, k_B Boltzmann's constant) by

$$n = 4\pi \left(\frac{2m_D^* k_b T}{h^2}\right)^{1.5} F_{\frac{1}{2}}(\eta)$$	(1)

where $F_i(\eta)$ is the Fermi integral of order i $F_i = \int_0^\infty \frac{\in^i d\in}{1+Exp[\in-\eta]}$. The reduced chemical potential can be extracted directly from the measured Seebeck coefficient value using

$$S = \pm\frac{k_B}{e}\left(\frac{2F_1(\eta)}{F_0(\eta)} - \eta\right)$$	(2)

while m_D^* is obtained from Eq (1) and the experimentally determined Hall coefficient R_H

$$R_H = \pm\frac{1}{en_H} = \pm\frac{r_H}{en},$$	(3)

n_H is denoted as Hall carrier concentration and the Hall scattering factor is only a function of η: $r_\mathrm{H} = \frac{3F_{0.5}(\eta)F_{-0.5}(\eta)}{4F_0^2(\eta)}$. Note that both S and R_H have a negative value if electrons are the relevant charge carrier and a positive value for holes.

The electrical conductivity is related to the carrier mobility μ by

$\sigma = en\mu$	(4)

which is related to the inertia or transport effective mass m_I^* by $\mu = e\tau/m_I^*$. For acoustic phonon scattering the experimentally determined Hall mobility $\mu_H = \mu * r_H$ is given by

$$\mu_{\mathrm{H,AP}} = \frac{F_{-0.5}}{2F_0}\frac{e\pi\hbar^4}{\sqrt{2}(kT)^{1.5}}\frac{C_l}{E_{\mathrm{def}}^2(m_I)(m_b^*)^{1.5}}$$	(5)

where E_{def} is the deformation potential, i.e. the scattering constant for AP scattering. $C_l = \rho {v_l}^2$ is the longitudinal elastic constant, related to the mass density ρ and the longitudinal speed of sound v_l. For the evaluation of Eq (5) it is assumed that the single valley effective mass m_b^* is identical to the transport effective mass m_I^*, which is strictly true only for materials with a spherical Fermi surface. In a system with degenerate bands, the (total) density of states effective mass m_D^* is related to the single valley mass by $m_D^* = N_v^{2/3} m_b^*$ where N_v is the valley degeneracy. If the elastic constant is known from literature, E_{def} can be obtained from the measured Hall mobility.

The measured total thermal conductivity is related to the lattice constant by

$\kappa = \kappa_{lat} + \kappa_e = \kappa_{lat} + \sigma T L(\eta)$	(6)
$$L = \frac{k_B^2}{e^2}\left(\frac{3F_0F_2 - 4F_1^2}{F_0^2}\right)$$	(7)

The system is thus fully described by $\kappa_{lat}(T)$, E_{def}, m_D^* (and possibly N_v) and all thermoelectric transport properties can be calculated as function of η(or n) and T.

For a system with two parabolic bands (2PB), the transport quantities are given by [50, 51]

$S = \frac{\sigma_1 S_1 + \sigma_2 S_2}{\sigma_1 + \sigma_2}$	(8)
$\sigma = \sigma_1 + \sigma_2$	(9)
$n = n_1 + n_2$	(10)
$R_H = \frac{R_{H1}\sigma_1^2 + R_{H2}\sigma_2^2}{(\sigma_1 + \sigma_2)^2} = \frac{n_{H,1}\mu_{H,1}^2 + n_{H,2}\mu_{H,2}^2}{e(n_{H,1}\mu_{H,1} + n_{H,2}\mu_{H,2})^2}$	(11)
$\kappa = \kappa_{lat} + \kappa_{e1} + \kappa_{e2} + \kappa_{e12}$	(12)

where the quantities $\sigma_i, S_i, R_{H,i}, n_i, \mu_{H,i}$ are given by Eqs. (1)-(5). The (single carrier type) electronic thermal conductivities are given by Eqs. (6) and (7) while the bipolar contribution κ_{e12} is given by $\kappa_{e12} = \frac{(S_1 - S_2)^2 \sigma_1 * \sigma_2}{\sigma_1 + \sigma_2} T$. Note that the single band equations are valid with respect to the chemical potential of that carrier type, i.e. $S_1 = S(\eta_1)$ and $S_2 = S(\eta_2)$, which are related to each other by the relative position of the bands with respect to each other. For the later considered case of two valence bands with the same maximum $\eta_1 = \eta_2 = \eta$, this also implies $\kappa_{e12} = 0$.

A SPB model is also often applied to material systems with a more complex band structure, e.g. with two or more valence or conduction bands with the extrema at the same energy level; relevant examples for this are $Mg_2Si_{1-x}Sn_x$ with $x \approx 0.65$ where the two lowest lying conduction band maxima converge [30-34, 52] or p-Mg_2X (*X*=Si, Ge, Sn) where the two or three highest valence bands all have their maximum at the same energy [26, 36, 37, 53-55]. In this case the bands are being treated as if they were truly identical/degenerate, i.e. the individual bands with $m_{b,i}^*$ are substituted by an average SPB mass, given by $m_D^* = N_v^{2/3} m_{b,SPB}^*$ [34, 54].

3. Results

In the following we'll compare the thermoelectric transport properties of a model system with two identical bands (SPB) and one with two bands with distinct effective masses (2PB). This allows evaluating the accuracy of assuming SPB-like behavior for a two band system. An variation of the bands with respect to each other in energy is not considered as this is easily recognized experimentally and it is clear the a single band model cannot be applied then [25].

To be able to calculate all the properties we'll use the physical parameters of p-Mg_2Sn, where some constants are reported and which is supposed to have two relevant VB according to [37]; nevertheless the numbers are not essential for the relevance of the following.

For a fair comparison, the m_D^* of both systems considered needs to be the same; this is essentially the same as saying that for a given carrier concentration the reduced chemical potential is identical in both systems. We take $m_D^* = 1.1\, m_0$ [54] for p-Mg_2Sn; m_0 is the free electron mass. The heavy hole and light hole valence bands clearly have different curvatures and we use the estimate of the effective mass ratio of $\frac{m_{HH}^*}{m_{LH}^*} := A \approx 4$ from the DFT calculation results in [37], similar to a recent result in [56]. As the total density of states effective mass is the weighted sum of the individual band

masses $m_D^* = \left(\sum m_i^{1.5}\right)^{2/3}$ it follows for our model system $m_{HH}^* = 1.02\, m_0, m_{LH}^* = 0.254\, m_0$. For the SPB system it follows from $m_D^* = N_v^{2/3} m_b^*$ with $N_v = 2$ $m_{b,SPB}^* = 0.69\, m_0$. The band structure is visualized in Figure 1a. Note that the effects of interband and intervalley scattering are not considered in the calculations. These could be different between the two considered systems [57], but intervalley scattering can usually be neglected if scattering by acoustic phonons is dominant [58], which tends to be true in thermoelectric materials above room temperature.

The thermoelectric properties for both SPB and 2PB system according to the equations given above are summarized in Figure 1b)-g). For these we have assumed the same deformation potential of $E_{Def} = 9$ eV for both bands in the 2PB system and the SPB system, the elastic constant as $C_l = 8.3 \times 10^{10}$ Pa [54, 59] and $\kappa_{lat}(300\ K) = 5.3$ W/mK [54].

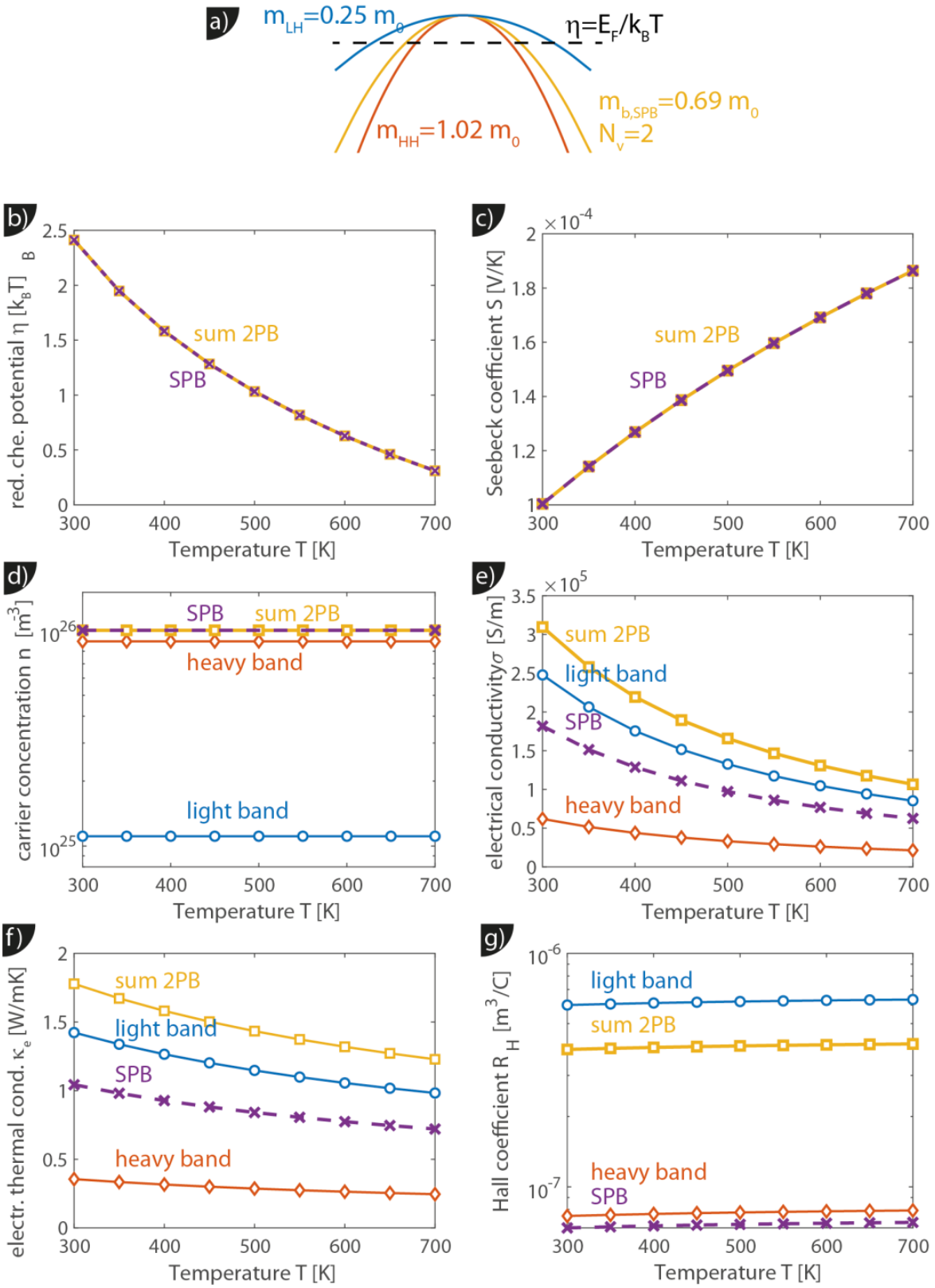

Figure 1: a) electronic band structure of a system with single, two-fold degenerate band (SPB) and one comprising a light and a heavy parabolic band that are degenerate only at the maxima (2PB). The band masses are designed such that the total density of states effective mass is the same in both cases. b)-g) Thermoelectric properties for the SPB and the 2PB system employing material constants for p-Mg_2Sn and $n = 10^{26}\ \mathrm{m}^{-3}$.

All properties are calculated for $n = 10^{26}\ \mathrm{m}^{-3}$. As can be seen from Figure 1b) the chemical potential is identical for both systems. This is due to having m_D^* identical for the two considered cases. As the Seebeck coefficient of the individual bands depends only on the chemical potential, it is also the same for all bands and hence for the 2PB and the SPB system. Figure 1d) shows the distribution of the carriers of the 2PB system. These are distributed according to $\frac{n_{HH}}{n_{LH}} = \left(\frac{m_{HH}^*}{m_{LH}^*}\right)^{1.5} = 8$ (Eq. (1)), i.e 89% are in the heavy valence band. For the SPB system the carriers are distributed equally (not shown) and the sum is of course the same in both systems. As we don't consider thermal excitation into the conduction band the carrier concentration is independent of temperature. As is clear from Figure 1e) the electrical conductivity of the 2PB system is significantly higher than that of the SPB system (≈70% in this case), even though n and m_D^* are identical. In fact, only the conductivity contribution from the LH band alone is larger than that of the SPB system with a two-fold degenerate band. The fundamental reason for that is the strong dependence of μ_H and hence σ on the band effective mass (Eq. (5)) which overcompensates the lower carrier concentration in the LH band; it is also due to keeping the scattering constant E_{Def} the same for all bands. As S is identical for both systems, this results in a significantly higher power factor for the 2PB system and is an example of the well-known fact, that a combination of dissimilar bands is favorable for optimizing thermoelectric properties [25, 48].

Perhaps the most important finding is that the Hall coefficient R_H is distinctly different; in this case $\frac{R_{H,2PB}}{R_{H,SPB}} \approx 6$ (Figure 1g). This is not necessarily surprising as Eq (3) and (11) are clearly different. While Eq (3) can be employed to calculate the carrier concentration from a (measured) Hall coefficient for a SPB system directly, Eq (10) would need to be involved for a 2PB system. Due to the interdependence of the 2-band properties the measured R_H *cannot* be directly translated into a carrier concentration [15]. If Eq (3) is employed on the 2PB system anyway this will lead to incorrect results. In the here considered case, the Hall coefficient of the 2PB system that would be measured is $R_{H,2PB} = 3.9 \times 10^{-7}\,\frac{m^3}{C}$. If Eq (3) is employed to calculate the carrier concentration, it will result in a Hall carrier concentration of $n_H = 1.6 \times 10^{25}\ m^{-3}$ and a carrier concentration of $n = 1.7 \times 10^{25}\ m^{-3}$, while the actual (input) carrier concentration is $n = 1 \times 10^{26}\ m^{-3}$. The difference between the "measured" and the true, input carrier concentration is not due to an error in the model or the calculation itself, but due to applying a model for a case where it cannot be applied. Essentially, if a single parabolic band analysis is applied for a 2PB system with the above properties, the carrier concentration is determined roughly a factor of 6 too small. Note that the Hall coefficient has a very weak temperature dependence as it is related to n_H which is linked to the temperature independent n by the Hall scattering factor $r_H(T)$.

As the carrier concentration is one of the basic properties on which an SPB analysis is usually based, this finding has severe implication for the SPB analysis as will be discussed later on. First however, we'll discuss how large the difference between the quantities in the SPB and the 2PB system is.

As derived in the appendix, ratios of SPB and 2PB quantities are relatively simple functions of the mass ratio $\frac{m_{b,1}^*}{m_{b,2}^*} = A$ (and partially N_v) only, i.e. independent of carrier concentration and other material specific constants. For the ratio of the electrical conductivities holds $\frac{\sigma_{2PB}}{\sigma_{SPB}} = \frac{(1+A)}{1}\frac{\left(1+A^{-1.5}\right)^{\frac{2}{3}}}{N_v^{5/3}}$

, i.e. the electrical conductivity of the 2PB system is always larger than that of the SPB system. For the Hall coefficient it can be shown that $\frac{R_{H,2PB}}{R_{H,SPB}} = \frac{(1+A^{-1.5})(1+A^{3.5})}{(1+A)^2}$; the Hall coefficient of the 2PB system is thus also always larger and the relative difference is even larger than for the electrical conductivity. We have visualized the contributions of the individual bands as well as the total electrical conductivity and Hall coefficient for the 2PB system normalized to the value of the SPB system in Figure 2a) and b). For $\frac{m^*_{b,1}}{m^*_{b,2}} = 1$ the band structures of the SPB and the 2PB are identical and the ratio is thus unity. With increasing mass ratio the total conductivities and Hall coefficients deviate, reaching a factor of 1.7 for the electrical conductivity and of 6 for the Hall coefficient for $\frac{m^*_{b,1}}{m^*_{b,2}} = 4$.

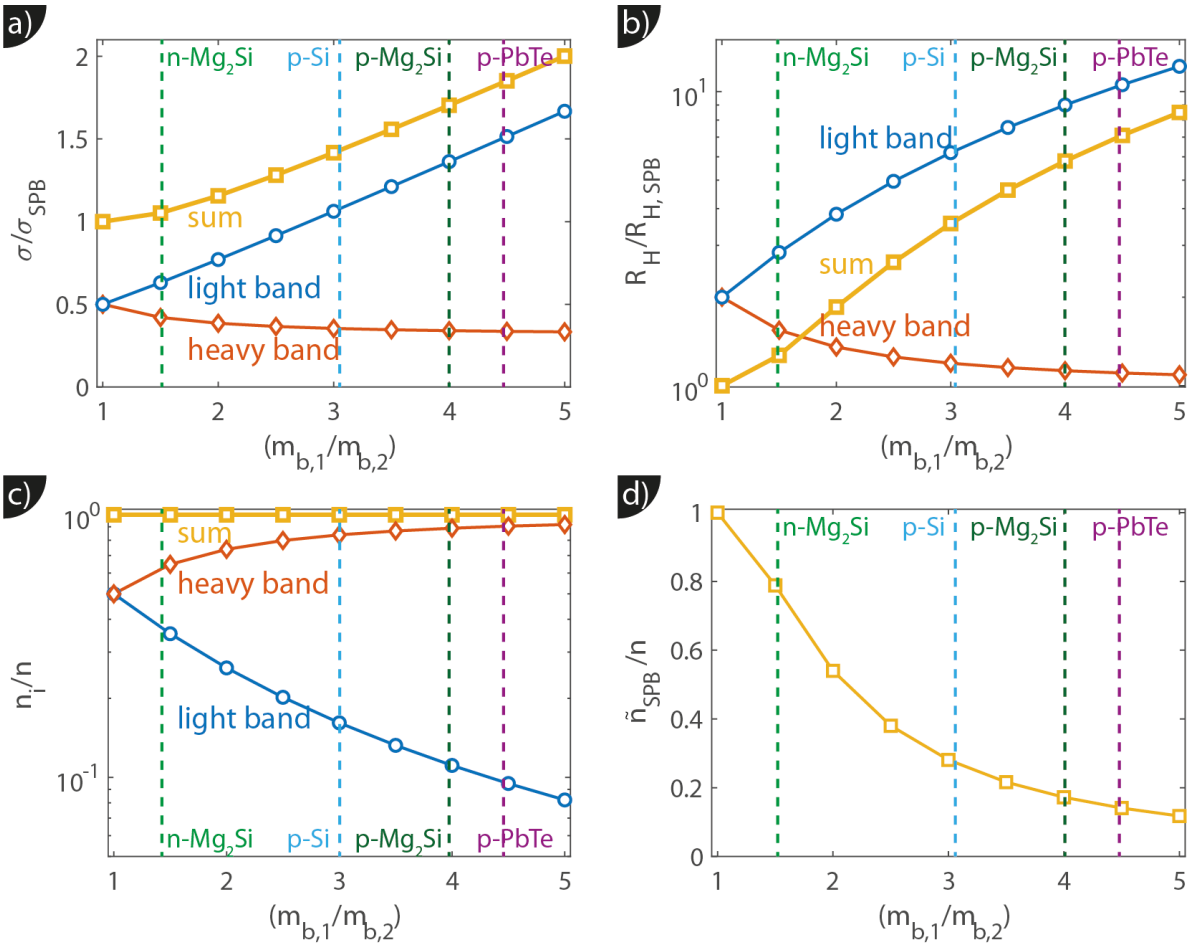

Figure 2: Electrical conductivity (a) and Hall coefficient (b) of a 2PB system normalized to the value of a SPB system with two identical bands as a function of the band effective mass ratio; all other physical constants are identical. c) Distribution of the charge carriers according to the mass ratio. d) Ratio of the carrier concentration calculated from $\frac{r_H}{R_H e}$ (assumption of SPB) and the true carrier concentration n. The band mass ratios estimated from literature for several materials are indicated as vertical lines.

Note that the difference of the power factor for the 2PB system is the same as for σ, since S is identical in both systems. With increasing mass ratio this overcompensates the decreasing fraction of light carriers which is plotted in Figure 2c and given by $n_2 = n\left(\frac{A^{-1.5}}{1+A^{-1.5}}\right)$. As the Hall coefficients of 2PB and SPB are quite different, using $n_H = \frac{1}{R_H e}$ (i.e. assuming SPB is valid), where R_H is the

experimentally measured value of the Hall coefficient, leads to an incorrect value of the carrier concentration $\tilde{n}_{SPB}$. Here the tilde indicates in the following quantities that are obtained if the validity of the SPB model is assumed and the corresponding equations are employed. As derived in Eq (A.2) the ratio of incorrectly determined carrier concentration and true carrier concentration is given by $\frac{\tilde{n}_{SPB}}{n} = \frac{R_{H,SPB}}{R_{H,2PB}} = \frac{(1+A)^2}{(1+A^{-1.5})(1+A^{3.5})}$. As can be seen from Figure 2d), even if the two band masses differ by only a factor of two, the carrier concentration is calculated a factor of two too small. We have also indicated the implications for different prominent thermoelectric material systems: for n-type $Mg_2Si_{1-x}Sn_x$ with $x \approx 0.6$ we have used $A = 1.45$ from Bahk et al. [11], somewhere in the middle of the values from other reports ($A = 1.35$ [30], $A = 1.13$ [60], $A = 2.4$ [61], $A = 1.6$ [50]). The large spread is due to different methods to extract the band masses from the available experimental or calculated data. Si also has a quite large mass ratio of $A = 3.1$ between the heavy and the light valence band [62], similar to p-Mg_2Sn. For PbTe we have indicated $A = \frac{0.6}{0.13} = 4.5$, although the heavy band mass is also estimated to be even higher in some of the reports [40]. Note that for PbTe the bands move with respect to each other with temperature and the calculation captures only the situation when the band maxima are aligned. The temperature at which this happens is disputed, but above room temperature [38-40, 47, 63].

4. Discussion

As shown in Figure 2d the experimentally obtained carrier concentration $\tilde{n}_{SPB}$ (assuming validity of the SPB model) is always smaller than the real one. This implies that under the taken assumptions the dopant efficiency (ratio of measured carrier concentration to carrier concentration expected from composition) is always obtained too small if the system studied has two bands which are not identical . Furthermore, comparison between different materials might be misleading if the band mass ratio differs between these. In the case of p-$Mg_2(Si,Sn)$ a decreasing dopant efficiency has been observed when going from Mg_2Sn to Mg_2Si and a difference between $Mg_2Si_{1-x}Sn_x$ and $Mg_2Ge_{1-x}Sn_x$ for the same x [26, 36]. This was deduced from the measured carrier concentration using $n_H = \frac{1}{R_H e}$. As indicated in Figure 1 the relevant bands are not identical and the material is therefore not truly SPB-like. It is therefore possible that the extent of the observed change in dopant efficiency is due to a change in $\frac{m^*_{b,1}}{m^*_{b,2}}$ when changing composition. Furthermore Figure 2d) also implies that carrier concentrations from Hall measurements can show only limited comparability when compared to results from other methods, as those results might be affected differently by the existence of distinct bands [64, 65].

As the carrier concentration is one of the most important inputs for the SPB analysis, the incorrectly obtained carrier concentration for a non-SPB system has implications for the analysis and the validity of the conclusions that can be drawn from it. Often the Pisarenko-plot $S(n)$ is used to check the validity of the assumed SPB model, to look for deviations and obtain an average value of m^*_D. Figure 3a) shows the Seebeck coefficient vs. the true carrier concentration n and vs. $\tilde{n}_{SPB}$. The physical constants are those of p-Mg_2Sn, i.e. the same as employed in Figure 1 and $\frac{m^*_{b,1}}{m^*_{b,2}} = 4$.

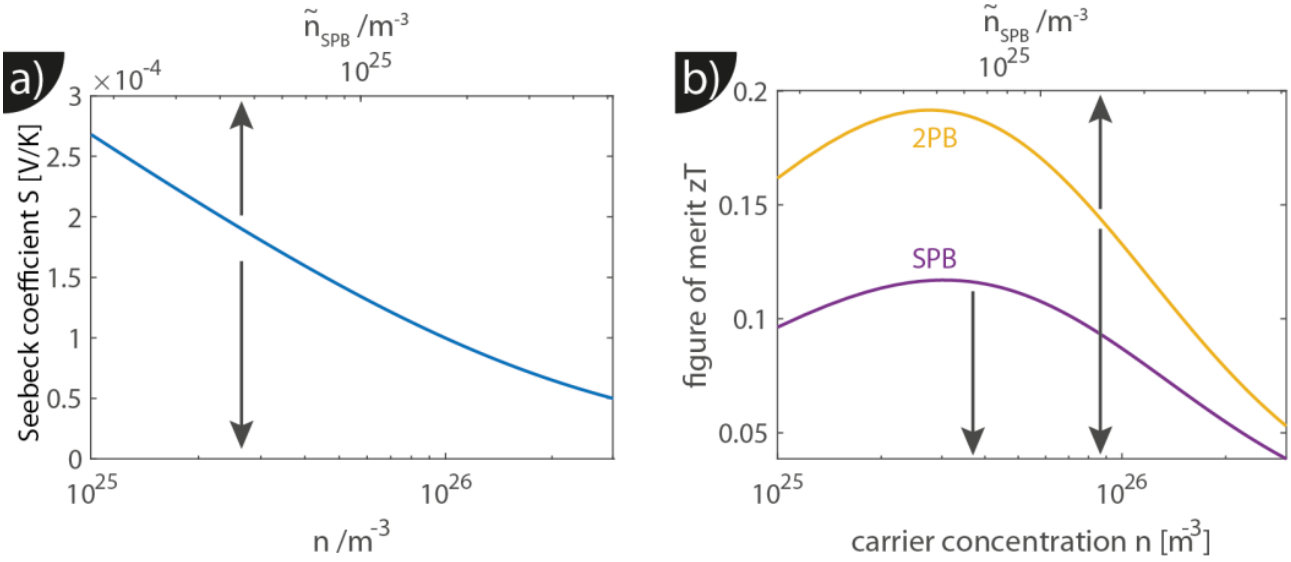

Figure 3: a) Seebeck coefficient at 300 K for a 2PB system with $\frac{m^*_{b,1}}{m^*_{b,2}} = 4$ (p-Mg_2Sn) over carrier concentration and "experimentally" determined carrier concentration $\tilde{n}_{SPB}$ if a single parabolic band model is assumed. b) Figure of merit at 300 K for the same 2PB system and the corresponding SPB system with $N_v = 2$. For the 2PB system the upper axis corresponds again to $\tilde{n}_{SPB}$.

As the error in carrier concentration is a constant factor, the incorrectly "experimentally" determined Pisarenko-plot is just shifted with respect to the correct one. If the density of states effective mass is determined using $\tilde{n}_{SPB}$, it is determined too small with $\frac{\tilde{m}^*_{D,SPB}}{m^*_D} = \left(\frac{\tilde{n}_{SPB}}{n}\right)^{2/3} \approx 0.3$, see Eq (1). This ratio is again independent of carrier concentration and experimentally the calculated $m^*_{D,SPB}$ will therefore not show any systematic deviations in the Pisarenko-plot. It is therefore not possible to identify a material system with two distinct, but degenerate bands from the Pisarenko-plot and the calculation of a too small density of states effective mass will happen unnoticed.
The deformation potential is calculated from the mobility and the effective mass. The effective mass is obtained incorrectly if SPB validity is assumed. This also holds for the mobility as it is obtained using the conductivity and the incorrect carrier concentration. As derived in Eq. A.7 $\frac{\tilde{E}_{Def,SPB}}{E_{Def}} = \left(\frac{\sigma_1 \tilde{n}_{SPB}\left(m^*_{b,1}\right)^{2.5}}{\sigma n_1 \left(\tilde{m}^*_{b,SPB}\right)^{2.5}}\right)^{1/2} = \frac{\left(1+A^{3.5}\right)^{2/6} N_v^{5/6}}{(1+A)^{7/6}}$, here $\tilde{m}^*_{b,SPB} = \tilde{m}^*{}_{D,SPB}/N_v^{2/3}$ is the (incorrect) band mass. For $A = 4 \Rightarrow \frac{\tilde{E}_{Def,SPB}}{E_{Def}} = 1.38$, i.e. the scattering potential is obtained 38% too large. This also implies that the value of $E_{Def} = 9\ eV$ which was taken from our previous work [54] is an effective, rather than the physically correct value for p-Mg_2X, as we had obtained it assuming an SPB model. However, the choice of the value does not affect the validity of the conclusions from comparing a SPB with a 2PB system. As for dopant activation and effective mass, comparability of the deformation potential between different materials and to the results of first principle calculations [66] is severely affected, even if the error is comparatively small.

A further fundamental parameter in the SPB description is κ_{lat}. For the SPB system holds $\kappa_{lat} = \kappa - \sigma_{SPB} L T$ while for the considered 2PB system Eq. (12) can be rewritten as $\kappa_{lat,2PB} = \kappa - LT(\sigma_1 + \sigma_2)$ with $L = L_1 = L_2$. If κ_{lat} is obtained by calculation using Eq. (4), (5) and Eq (9) the calculated lattice thermal conductivity will be different for the systems as the calculated electrical conductivities are different. However, the (total) electrical conductivity is typically measured and for both systems

holds $\kappa_{lat} = \kappa - \sigma_{tot} LT$. Thus, if the measured electrical conductivity is employed the result for the lattice thermal conductivity is the same for both systems and employing SPB does not result in incorrect values."

Material parameters that are derived from m_D^* and E_{Def}, like $\beta = \frac{\left(\frac{m_D^*}{m_0}\right)^{1.5} \mu_0 \, T^{2.5}}{\kappa_{lat}}$, the weighted mobility $u = \left(\frac{m_D^*}{m_0}\right)^{1.5} \mu_0$ and the B-factor $B = \frac{2k_B^2 \hbar}{3\pi} \frac{N_v C_l T}{m_i^* E_{Def}^2 \kappa_{lat}}$ (for acoustic phonon scattering) and that are used to compare materials with each other [31, 47, 52, 67-69] are consequently also calculated incorrectly if the considered bands in a material are not identical.

Figure 3b) compares zT for the SPB and 2PB system, the result for the 2PB system is also shown as function of $\tilde{n}_{SPB}$. First it can be seen that the 2PB system has a higher figure of merit, this is due to the enhancement of the electrical conductivity due to the light band, partially compensated by an increase in κ due to the higher electronic contribution. Second, zT vs. the upper x-axis would be the experimentally obtained result if the carrier concentration is obtained assuming a SPB system. This highlights again that the experimentally predicted optimum carrier concentration is far off the real optimum. However, as the error depends on the band mass ratio but is independent of n, the plot can still be used to predict zT for different $\tilde{n}_{SPB}$ and thus estimate the maximum figure of merit of a material system, even if the absolute values for the carrier concentration are incorrect. Third, the shape of the SPB and the 2PB curve are basically the same, it is therefore not possible to distinguish a 2PB from a SPB system from either the experimental $S(n)$ or $zT(n)$ plots. From the used set of parameters it also appears that the optimum carrier concentration are practically identical for the SPB and the 2PB system.

Note that the main point of the comparison between the SPB and the 2PB system is to visualize potential shortcomings of the usage of the SPB model. Employing a 2PB model does not necessarily give a fully correct description as the results obtained were derived under the assumption that the deformation potential is the same for all bands considered. This is often assumed in literature and used to derive the well known $\frac{\mu_{H,1}}{\mu_{H,2}} = \left(\frac{m_{b,1}^*}{m_{b,2}^*}\right)^{-2.5}$ relation [16, 47, 70], but it is not clear that this is always fulfilled for real material systems. Especially for material systems where the band convergence of two distinct bands is achieved by a variation of temperature or composition [25, 61], the assumption that these two bands will have the same deformation potential is not well justfified. In that case the extend of the discussed inaccuracies due to assuming SPB for a more complex band structure will depend on the ratio of the deformation potentials for the respective bands.

5. Conclusion

We have calculated the thermoelectric properties for a system with two identical bands and a system with two bands that are degenerate at the band maximum but have different effective masses; the total density of states effective mass is identical. The former is effectively a single parabolic band system while the latter is not. Calculation of the thermoelectric properties for the same carrier concentration, same interaction parameters and adjusted band masses shows that electrical conductivity, power factor and Hall coefficient are not the same. This originates from the strong dependence of the mobility on the band masses (and due to keeping the scattering potentials

constant). We show that in particular the Hall coefficient is sensitive to the band masses and differs significantly between a SPB and 2PB system.

Experimental transport data is often analyzed assuming a SPB model to be valid and used for material optimization and the calculation of fundamental material properties. We have therefore analyzed the outcome of such an SPB analysis on a 2PB system. It is shown that the carrier concentration is obtained too low; for a material system with a band mass ratio of 4 (comparable to p-PbTe, p-Mg_2Sn and p-Si) by a factor of 6. Therefore, also the density of states effective mass is determined too small (factor of 3) and the acoustic phonon scattering constant too large (factor of 1.4). We have furthermore shown that the errors can be expressed as analytical functions of the band mass ratio. This implies that the optimum carrier concentration, the dopant efficiencies, the effective mass and the scattering constant are obtained incorrectly and cannot be compared directly with results from other methods, e.g. DFT. Furthermore, this limits the comparability of the SPB analysis for different material classes as the band mass ratios are usually material specific. As the error is independent of carrier concentration it is not possible to tell from the usual transport data only, e.g. Pisarenko-plot or $zT(n)$, if a system is truly SPB or not. On the other hand the prediction of the optimum figure of merit from a few experimental values is still approximately correct as is the determined lattice conductivity.

The conclusion drawn were obtained by comparing a SPB system with two identical bands and a true 2PB system, where the bands have different masses, assuming scattering by acoustic phonons to be dominant. However, the general conclusion that performing an SPB analysis can lead to significant errors in carrier concentration and material constants is not restricted to a 2PB system, but will hold also for more complex band structures and other scattering mechanisms or combinations of those. Essentially, usage of an SPB description for a more complex system can lead to a self-consistent description of the material and the SPB model can therefore be used for an optimization with respect to carrier concentration. However, the obtained material constants will not be correct, which heavily limits comparability between different material systems. This shows that the results of an SPB analysis have to be taken with care, and while its use is undisputed, it is also clearly limited.

Acknowledgements

The author would like to gratefully acknowledge the endorsement from the German Aerospace Center (DLR), Germany Executive Board Member for Space Research and Technology and the financial support from the Young Research Group Leader Program as well as financial support by the Deutscher Akademischer Austauschdienst-Department of Science Technology (DAAD-DST), Germany-India collaboration (Project ID: 57317956) and Deutsche Forschungsgemeinschaft (DFG, German Research Foundation) project number 396709363. Finally, I'd like to thank Prof. Titas Dasgupta (IIT Bombay) for insightful discussion.

Appendix

For all the following calculations relations between the SPB, the total and the individual band quantities are required. These can be expressed naturally as functions of $A \coloneqq \frac{m_{1,b}^*}{m_{2,b}^*}$. For the band masses hold:

$\left(m_{b,1}^*\right)^{1.5} = (m_D^*)^{1.5} - (m_{b,2}^*)^{1.5} \Rightarrow m_{b,1}^* = \frac{m_D^*}{(1+A^{-1.5})^{2/3}}$	A.1

For the carrier concentrations hold

$\frac{n_1}{n_2} = \frac{n_{H,1}}{n_{H,2}} = \left(\frac{m_{b,1}^*}{m_{b,2}^*}\right)^{1.5} = A^{1.5}$ and $n = n_1(1+A^{-1.5})$	A.2

as the Fermi integrals in Eq. (1) cancel due to the same η for all bands.
Under the assumption that C_l and E_{Def} are identical follows from Eq. (5)

$\frac{\mu_{H,1}}{\mu_{H,2}} = \frac{\mu_1}{\mu_2} = \left(\frac{m_{b,1}^*}{m_{b,2}^*}\right)^{-2.5} := A^{-2.5}$ and $\frac{\mu_1}{\mu_{SPB}} = \frac{\left(1+A^{-1.5}\right)^{\frac{5}{3}}}{N_v^{5/3}}$	A.3

From this the relation between the conductivities can be derived:

$\frac{\sigma_{2PB}}{\sigma_{SPB}} = \frac{\sigma_1+\sigma_2}{\sigma_{SPB}} = \frac{n_1\mu_1 + n_2\mu_2}{n\mu_{SPB}} = \frac{n_1\mu_1 + n_1A^{-1.5}\mu_1A^{2.5}}{n_1(1+A^{-1.5})\mu_{SPB}}$ $= \frac{\mu_1(1+A)}{(1+A^{-1.5})\mu_{SPB}} = \frac{(1+A)}{1}\frac{(1+A^{-1.5})^{\frac{2}{3}}}{N_v^{5/3}}$	A.4

Which gives ≈ 1.7 for $A = 4$ as can be seen in Figure 1. Similarly $\frac{\sigma_1}{\sigma_{2PB}} = \frac{1}{1+A}$. For the Hall coefficient holds

$\frac{R_{H,SPB}}{R_{H,2PB}} = \frac{\frac{1}{en_H}}{\frac{+n_{H,1}\mu_{H,1}^2 + n_{H,2}\mu_{H,2}^2}{e\left(n_{H,1}\mu_{H,1} + n_{H,2}\mu_{H,2}\right)^2}} = \frac{(1+A)^2}{(1+A^{-1.5})(1+A^{3.5})}$	A.5

If the SPB analysis is used for a system with two bands with different masses the SPB parameters are obtained incorrectly. For the carrier concentration holds $\tilde{n}_{SPB} = \frac{1}{R_{H,2PB}}$ where $\tilde{n}_{SPB}$ is the (incorrect) carrier concentration obtained assuming SPB. On the other hand, if a system follows SPB strictly, then $n = n_{SPB} = \frac{1}{R_{H,SPB}}$, i.e. $\frac{\tilde{n}_{SPB}}{n} = \frac{R_{H,SPB}}{R_{H,2PB}}$ (see Eq. A.5) which means that the carrier concentration is determined too small.

The effective mass is effectively determined from Eq (1) using $n \propto (m_D^*)^{1.5}$. If $\tilde{n}_{SPB}$ is employed it follows

$\frac{\tilde{m}^*{}_{D,SPB}}{m_D^*} = \left(\frac{\tilde{n}_{SPB}}{n}\right)^{2/3} = \left(\frac{(1+A)^2}{(1+A^{-1.5})(1+A^{3.5})}\right)^{2/3}$	A.6

For a 2PB holds $E_{Def} \propto \left(\frac{1}{\mu_1\left(m_{b,1}^*\right)^{2.5}}\right)^{1/2} \propto \left(\frac{1}{\mu_2\left(m_{b,2}^*\right)^{2.5}}\right)^{1/2}$. If SPB is assumed the deformation potential will be obtained (incorrectly) from $\tilde{E}_{Def,SPB} = \left(\frac{C}{\tilde{\mu}_{SPB}\left(\tilde{m}_{b,SPB}^*\right)^{2.5}}\right)^{1/2}$ where the $\tilde{\mu}_{SPB}$ is calculated from electrical conductivity and (incorrect) carrier concentration, i.e. $\tilde{\mu}_{SPB} = \frac{\sigma}{e\tilde{n}_{SPB}}$. As the density of states mass is determined incorrectly (see Eq. A.6) the band mass is as well, with $\tilde{m}_{b,SPB}^* =$

$\widetilde{m}^*_{D,SPB}/N_v^{2/3}$. For the deformation potential ratio therefore holds

$$\frac{\tilde{E}_{Def,SPB}}{E_{Def}} = \left(\frac{\mu_1 (m^*_{b,1})^{2.5}}{\tilde{\mu}_{SPB}(\widetilde{m}^*_{b,SPB})^{2.5}}\right)^{1/2} = \left(\frac{\sigma_1 \tilde{n}_{SPB}(m^*_{b,1})^{2.5}}{\sigma n_1 (\widetilde{m}^*_{b,SPB})^{2.5}}\right)^{1/2}.$$

With $\frac{\sigma_1}{\sigma} = \frac{1}{1+A}$, $\frac{\tilde{n}_{SPB}}{n_1} = \frac{(1+A)^2}{(1+A^{3.5})}$ (from Eq. A.5 and $n_1 = \frac{n}{1+A^{-1.5}}$) and

$\frac{\tilde{n}_{SPB}}{n} = \frac{(1+A)^2}{(1+A^{-1.5})(1+A^{3.5})}$ and $n_1 = \frac{n}{1+A^{-1.5}} \Rightarrow \frac{\tilde{n}_{SPB}}{n_1} = \frac{(1+A)^2}{(1+A^{3.5})}$ and $\frac{m^*_{b,1}}{\widetilde{m}^*_{b,SPB}} = \frac{m^*_D}{(1+A^{-1.5})^{2/3}} \frac{N_v^{2/3}}{\widetilde{m}^*_{D,SPB}} = \frac{(1+A^{3.5})^{2/3}}{1} \frac{N_v^{2/3}}{(1+A)^{4/3}}$ follows

$\frac{\tilde{E}_{Def,SPB}}{E_{Def}} = \frac{(1+A^{3.5})^{2/6} N_v^{5/6}}{(1+A)^{7/6}}$	A.7

References

1. Bell, L.E., *Cooling, Heating, Generating Power, and Recovering Waste Heat with Thermoelectric Systems.* Science, 2008. **321**(5895): p. 1457-1461.
2. Snyder, G.J. and E.S. Toberer, *Complex thermoelectric materials.* Nat Mater, 2008. **7**(2): p. 105-14.
3. He, W., et al., *Recent development and application of thermoelectric generator and cooler.* Appl Energ, 2015. **143**: p. 1-25.
4. Kresse, G. and J. Furthmüller, *Efficiency of ab-initio total energy calculations for metals and semiconductors using a plane-wave basis set.* Computational Materials Science, 1996. **6**(1): p. 15-50.
5. Kresse, G. and J. Furthmüller, *Efficient iterative schemes for ab initio total-energy calculations using a plane-wave basis set.* Phys. Rev. B, 1996. **54**(16): p. 11169-11186.
6. Madsen, G.K.H. and D.J. Singh, *BoltzTraP. A code for calculating band-structure dependent quantities.* Comput. Phys. Commun., 2006. **175**(1): p. 67-71.
7. Ryu, B., et al., *Hybrid-Functional and Quasi-Particle Calculations of Band Structures of Mg2Si, Mg2Ge, and Mg2Sn.* J Kor Phys Soc, 2019. **75**(2): p. 144-152.
8. Carrete, J., et al., *Finding Unprecedentedly Low-Thermal-Conductivity Half-Heusler Semiconductors via High-Throughput Materials Modeling.* Phys. Rev. X, 2014. **4**(1): p. 9.
9. Wang, X., et al., *Identification of Crystalline Materials with Ultra-Low Thermal Conductivity Based on Machine Learning Study.* The Journal of Physical Chemistry C, 2020. **124**(16): p. 8488-8495.
10. Wang, T., et al., *Cu3ErTe3: a new promising thermoelectric material predicated by high-throughput screening.* Materials Today Physics, 2020. **12**: p. 7.
11. Bahk, J.H., Z.X. Bian, and A. Shakouri, *Electron transport modeling and energy filtering for efficient thermoelectric Mg2Si1-xSnx solid solutions.* Phys. Rev. B, 2014. **89**(7): p. 075204.
12. Kim, H.-S., et al., *Characterization of Lorenz number with Seebeck coefficient measurement.* APL Mater., 2015. **3**(4): p. 041506.
13. Mao, J., W. Liu, and Z. Ren, *Carrier distribution in multi-band materials and its effect on thermoelectric properties.* Journal of Materiomics, 2016. **2**(2): p. 203-211.

14. Pei, Y.Z., A.F. May, and G.J. Snyder, *Self-Tuning the Carrier Concentration of PbTe/Ag2Te Composites with Excess Ag for High Thermoelectric Performance.* Adv. Energy Mater., 2011. **1**(2): p. 291-296.
15. Jaworski, C.M., et al., *Valence-band structure of highly efficient p-type thermoelectric PbTe-PbS alloys.* Phys. Rev. B, 2013. **87**(4): p. 045203.
16. Fistul, V.I., *Heavily Doped Semiconductors*. Monographs in Semiconductor Physics. Vol. 1. 1969: Springer.
17. Bux, S.K., et al., *Mechanochemical synthesis and thermoelectric properties of high quality magnesium silicide.* J. Mater. Chem., 2011. **21**(33): p. 12259-12266.
18. May, A.F., E. Flage-Larsen, and G.J. Snyder, *Electron and phonon scattering in the high-temperature thermoelectric La3Te4-zMz (M=Sb,Bi).* Phys. Rev. B, 2010. **81**(12).
19. May, A.F., *High-Temperature Transport in Lanthanum Telluride and Other Modern Thermoelectric Materials*, in *Chemistry and Chemical Engineering* 2010, California Institute of Technology.
20. May, A.F., et al., *Characterization and analysis of thermoelectric transport in n-type Ba8Ga16-xGe30+x.* Phys. Rev. B, 2009. **80**(12).
21. de Boor, J., et al., *Microstructural effects on thermoelectric efficiency: A case study on magnesium silicide.* Acta Mater., 2014. **77**(0): p. 68-75.
22. Wu, D., et al., *Superior thermoelectric performance in PbTe–PbS pseudo-binary: extremely low thermal conductivity and modulated carrier concentration.* Energ Environ Sci, 2015. **8**(7): p. 2056-2068.
23. Kamila, H., et al., *Non-Rigid Band Structure in Mg2Ge for Improved Thermoelectric Performance.* Advanced Science, 2020. **n/a**(n/a): p. 2000070.
24. Naithani, H. and T. Dasgupta, *Critical Analysis of Single Band Modeling of Thermoelectric Materials.* ACS Appl Energ Mat, 2020. **3**(3): p. 2200-2213.
25. Tang, Y., et al., *Convergence of multi-valley bands as the electronic origin of high thermoelectric performance in CoSb3 skutterudites.* Nat. Mater., 2015. **14**: p. 1223.
26. de Boor, J., et al., *Recent progress in p-type thermoelectric magnesium silicide based solid solutions.* Materials Today Energy, 2017. **4**: p. 105-121.
27. de Boor, J., T. Dasgupta, and E. Mueller, *Thermoelectric Properties of Magnesium Silicide Based Solid Solutions and Higher Manganese Silicides*, in *Materials Aspect of Thermoelectricty*, C. Uher, Editor. 2016, Taylor & Francis.
28. Wood, M., et al., *Observation of valence band crossing: the thermoelectric properties of CaZn2Sb2-CaMg2Sb2 solid solution.* Journal of Materials Chemistry A, 2018. **6**(20): p. 9437-9444.
29. Wang, H., et al., *The Criteria for Beneficial Disorder in Thermoelectric Solid Solutions.* Adv. Funct. Mater., 2013. **23**(12): p. 1586-1596.
30. Liu, W., et al., *Convergence of Conduction Bands as a Means of Enhancing Thermoelectric Performance of n-Type Mg2Si1-xSnx Solid Solutions.* Phys. Rev. Lett., 2012. **108**(16): p. 166601.
31. Mao, J., et al., *Thermoelectric properties of materials near the band crossing line in Mg2Sn–Mg2Ge–Mg2Si system.* Acta Mater., 2016. **103**: p. 633-642.
32. Zaitsev, V.K., et al., *Thermoelectrics on the Base of Solid Solutions of Mg2B IVCompounds*, in *Thermoelectrics Handbook: Macro to Nano*, D.M. Rowe, Editor. 2005, CRC: Boca Raton, USA.
33. Dasgupta, T., et al., *Influence of power factor enhancement on the thermoelectric figure of merit in Mg2Si0.4Sn0.6based materials.* physica status solidi (a), 2014. **211**(6): p. 1250-1254.
34. Liu, W., et al., *Advanced thermoelectrics governed by a single parabolic band: Mg2Si(0.3)Sn(0.7), a canonical example.* Phys Chem Chem Phys, 2014. **16**(15): p. 6893-7.
35. Zhang, Q., et al., *Low effective mass and carrier concentration optimization for high performance p-type Mg2(1-x)Li2xSi0.3Sn0.7 solid solutions.* PCCP, 2014. **16**(43): p. 23576-23583.
36. de Boor, J., et al., *Thermoelectric performance of Li doped, p-type Mg2(Ge,Sn) and comparison with Mg2(Si,Sn).* Acta Mater., 2016. **120**: p. 273-280.

37. Kutorasinski, K., et al., *Importance of relativistic effects in electronic structure and thermopower calculations for Mg2Si, Mg2Ge, and Mg2Sn.* Phys. Rev. B, 2014. **89**(11): p. 115205-1-8.
38. Zhao, L.D., V.P. Dravid, and M.G. Kanatzidis, *The panoscopic approach to high performance thermoelectrics.* Energ Environ Sci, 2014. **7**(1): p. 251-268.
39. Pei, Y., et al., *Convergence of electronic bands for high performance bulk thermoelectrics.* {NATURE}, 2011. **{473}**({7345}): p. {66-69}.
40. Jaworski, C.M., et al., *Valence-band structure of highly efficient <math><mi>p</mi></math>-type thermoelectric PbTe-PbS alloys.* Phys. Rev. B, 2013. **87**(4): p. 045203.
41. Bux, S.K., et al., *Nanostructured Bulk Silicon as an Effective Thermoelectric Material.* Adv. Funct. Mater., 2009. **19**: p. 2445-2452.
42. Schierning, G., et al., *Role of oxygen on microstructure and thermoelectric properties of silicon nanocomposites.* {JOURNAL OF APPLIED PHYSICS}, 2011. **{110}**({11}).
43. de Boor, J., et al., *Thermoelectric properties of porous silicon.* Appl. Phys. A, 2012. **107**: p. 789-794.
44. Shi, X., et al., *Extraordinary n-Type Mg3SbBi Thermoelectrics Enabled by Yttrium Doping.* 2019. **31**(36): p. 1903387.
45. Zhang, J., et al., *Discovery of high-performance low-cost n-type Mg3Sb2-based thermoelectric materials with multi-valley conduction bands.* Nat Commun, 2017. **8**(1): p. 13901.
46. Fu, C., et al., *Band engineering of high performance p-type FeNbSb based half-Heusler thermoelectric materials for figure of merit zT > 1.* Energ Environ Sci, 2015. **8**(1): p. 216-220.
47. Zhu, T., et al., *Compromise and Synergy in High-Efficiency Thermoelectric Materials.* Adv. Mater., 2017: p. 1605884-n/a.
48. Pei, Y., H. Wang, and G.J. Snyder, *Band Engineering of Thermoelectric Materials.* Adv. Mater., 2012. **24**(46): p. 6125-6135.
49. May, A.F. and G.J. Snyder, *Introduction to Modeling Thermoelectric Transport at High Temperatures*, in *Thermoelectrics and its Energy Harvesting: Materials, Preparation, and Characterization in Thermoelectrics*, D.M. Rowe, Editor. 2012, CRC Press.
50. Zhang, L., et al., *Suppressing the bipolar contribution to the thermoelectric properties of Mg2Si0.4Sn0.6 by Ge substitution.* J. Appl. Phys., 2015. **117**(15): p. 155103.
51. Nolas, G.S., J. Sharp, and J. Goldsmid, *Thermoelectrics: Basic Principles and New Materials Developments*. Vol. 45. 2001: Springer.
52. Liu, X.H., et al., *Low Electron Scattering Potentials in High Performance Mg2Si0.45Sn0.55 Based Thermoelectric Solid Solutions with Band Convergence.* Adv. Energy Mater., 2013. **3**(9): p. 1238-1244.
53. Bourgeois, J., et al., *Study of electron, phonon and crystal stability versus thermoelectric properties in Mg2X(X = Si, Sn) compounds and their alloys.* Functional Materials Letters, 2013. **06**(05): p. 1340005.
54. Kamila, H., et al., *Analyzing transport properties of p-type Mg2Si–Mg2Sn solid solutions: optimization of thermoelectric performance and insight into the electronic band structure.* Journal of Materials Chemistry A, 2019. **7**(3): p. 1045-1054.
55. Saparamadu, U., et al., *Comparative studies on thermoelectric properties of p-type Mg2Sn0.75Ge0.25 doped with lithium, sodium, and gallium.* Acta Mater., 2017. **141**: p. 154-162.
56. de Boor, J., A. Berche, and P. Jund, *Density of States Effective Mass for p-Type Mg2Si-Mg2Sn Solid Solutions: Comparison between Experiments and First Principles Calculations.* The Journal of Physical Chemistry C, 2020.
57. Witkoske, E., et al., *Thermoelectric band engineering: The role of carrier scattering.* 2017. **122**(17): p. 175102.
58. Norouzzadeh, P. and D. Vashaee, *Classification of Valleytronics in Thermoelectricity.* Sci Rep, 2016. **6**(1): p. 22724.

59. Klobes, B., et al., *Lattice dynamics and elasticity in thermoelectric Mg2Si1−xSnx.* Phys. Rev. Mater., 2019. **3**(2): p. 025404.
60. Pshenai-Severin, D.A., M.I. Fedorov, and A.Y. Samunin, *The Influence of Grain Boundary Scattering on Thermoelectric Properties of Mg2Si and Mg2Si0.8Sn0.2.* J. Electron. Mater., 2013. **42**: p. 1707-1710.
61. Zaitsev, V.K., et al., *Highly effective Mg2Si1-xSnx thermoelectrics.* Phys. Rev. B, 2006. **74**(4): p. 045207.
62. Zeghbroeck, B.V., *Principles of Semiconductor Devices.* 2011.
63. Cao, J., et al., *Thermally induced band gap increase and high thermoelectric figure of merit of n-type PbTe.* Materials Today Physics, 2020. **12**: p. 10.
64. Spitzer, W.G. and J.M. Whelan, *Infrared Absorption and Electron Effective Mass in n-Type Gallium Arsenide.* Physical Review, 1959. **114**(1): p. 59-63.
65. Pickering, C., *Infrared reflectivity measurements on bulk and epitaxial GaSb. (Carrier concentration and mobility measurements).* Journal of Physics C: Solid State Physics, 1980. **13**(15): p. 2959-2968.
66. Murphy-Armando, F. and S. Fahy, *First-principles calculation of carrier-phonon scattering in n-type ${\text{Si}}_{1\ensuremath{-}x}{\text{Ge}}_{x}$ alloys.* Phys. Rev. B, 2008. **78**(3): p. 035202.
67. de Boor, J., et al., *Thermoelectric transport and microstructure of optimized Mg2Si0.8Sn0.2.* J. Mater. Chem. C, 2015. **3**(40): p. 10467-10475.
68. Kamila, H., et al., *Systematic analysis of the interplay between synthesis route, microstructure, and thermoelectric performance in p-type Mg2Si0.2Sn0.8.* Materials Today Physics, 2019: p. 100133.
69. Snyder, G.J., et al., *Weighted Mobility.* **n/a**(n/a): p. 2001537.
70. Winkler, U.E., *Die elektrischen Eigenschaften der intermetallischen Verbindungen Mg2Si, Mg2Ge, Mg2Sn und Mg2Pb*. 1955, Eidgenoessische Technische Hochschule in Zuerich: Buchdruckerei Birkhäuser AG, Basel.